

# Comparison of the Viscous and Elastic Components of Two ABS Materials with Creep, Stress Relaxation and Constant Strain Rate Measurements Using the Universal Viscoelastic Model

Richard D. Sudduth

Materials Research and Processing Consultants, 102 Rue Le Bois, Lafayette, Louisiana 70508

Received 15 November 2002; accepted 18 February 2003

**ABSTRACT:** In general, the universal viscoelastic model evaluated in this study was found to adequately predict constant strain rate, creep, and/or stress relaxation measurements from the constants determined from constant strain rate measurements. The elastic and viscous components for two acrylonitrile–butadiene–styrene (ABS) viscoelastic materials were also easily isolated using this new universal viscoelastic model. The creep measurements for ABS-A (25383-A) and ABS-N (LL-4102-N) at three different stresses allowed elucidation of the common creep intercept strain of the calculated creep slopes that was designated as the “projected elastic limit.” Once the values for  $n$  and  $\beta$  were evaluated from creep measurements, then the creep variation of the universal viscoelastic model yielded a reasonably good fit of the measured creep data for both ABS-A and ABS-N. The extensional viscosity constant  $\lambda_E$  was found to be 7.2% greater for ABS-A than for ABS-N. Consequently, ABS-N was found to have a lower extensional viscosity in secondary creep than that of ABS-A at any specific strain rate. The value of the efficiency of yield energy dissipation  $n$  for ABS-N as determined from creep measurements was also 37.6% larger than the value of  $n$  for ABS-A. In addition, the

projected elastic limit  $\epsilon_c$  for ABS-A was 2% greater than the projected elastic limit for ABS-N. These observations indicated that ABS-A should be slightly more solidlike than ABS-N. However, both ABS-A and ABS-N were significantly more solidlike than liquidlike because both of their values for the efficiency of yield energy dissipation  $n$  were very close to zero. In general, values of  $n$  range from  $0 < n < 1$  with a material characterized as being essentially pure elastic having a value of  $n = 0$ . Using the yield strain as the failure condition for constant strain rate and stress relaxation measurements and the strain at critical creep, the failure condition for creep, it was found that the universal viscoelastic model allowed these failure criteria to yield remarkably good agreement on a projected time scale. This agreement resulted even though separate and independent data were used to evaluate these three different techniques for both ABS-A and ABS-N. © 2003 Wiley Periodicals, Inc. *J Appl Polym Sci* 90: 1298–1318, 2003

**Key words:** viscoelastic properties; stress; strain; creep; energy dissipation

## INTRODUCTION

Recently a series of articles have been written by this author<sup>1–5</sup> characterizing a new universal viscoelastic model that describes a definitive relationship between constant strain rate, creep, and stress relaxation analysis for viscoelastic polymeric compounds. This model also incorporates several new concepts to describe what we mean by viscoelasticity. The second article<sup>2</sup> in this series introduced a new term described as the efficiency of yield energy dissipation  $n$ , which has been found to directly characterize the viscous or elastic character of a material. In general, it has been found that the efficiency of yield energy dissipation appears to range primarily from  $0 < n < 1$ . In this range a material would be characterized as being essentially pure elastic if it were to have an efficiency of

yield energy dissipation value of  $n = 0$ . A material characterized as being primarily viscous in character would have an efficiency of yield energy dissipation value of  $n = 1$ . This new concept of viscoelasticity has been found to be consistent with the earlier efforts of Scott-Blair<sup>6</sup> as well as the more recent efforts of Hernandez et al.<sup>7</sup>

The isolation of additional direct measures of the elastic and viscous components of a viscoelastic material has also been recently shown<sup>4,5</sup> to be easily attainable using this new model. In particular, the concept of a “projected elastic limit” as determined from secondary creep measurements has been shown<sup>4</sup> to be directly obtainable using this new universal viscoelastic model. In addition, the extensional viscosity has also been found to be directly characterizable from secondary creep measurements using a new power law relationship. A discussion of how to obtain both the elastic and viscous components of a material from this model is described in some detail in this study from the constant strain rate and creep measurements

Correspondence to: richsudduth@earthlink.net.

characterized for two acrylonitrile-butadiene-styrene (ABS) materials.

In recent years the need for a simple analysis approach that relates creep, stress relaxation, and constant strain rate measurements all in one simple model has been generated as a result of the extended use of finite element analysis involving polymeric compounds<sup>8</sup> and composites.<sup>9</sup> Before the introduction of this new universal viscoelastic model several authors had attempted to describe two or more of these viscoelastic concepts in one unifying formulation.<sup>10,11</sup> However, most of the effort over the years has been to simulate uniaxial creep,<sup>12,13</sup> stress relaxation,<sup>10</sup> or constant strain rate data<sup>14-17</sup> separately. This new formulation approach offers a reasonably simple process in which to shift from a constant strain rate configuration to a creep calculation or stress relaxation configuration without changing formulation considerations or without stress or strain discontinuities.

This universal viscoelastic model has also been extended<sup>2-5</sup> to better understand the similarities between the failure criteria characteristics involving creep, constant strain rate, and stress relaxation. The relationship of the failure criteria among these three different techniques for characterizing a viscoelastic material is addressed in this study by use of the constant strain rate creep and stress relaxation measurements for two different ABS materials. For reference, this new universal viscoelastic model<sup>1-5</sup> is briefly reviewed before discussing the physical property measurements using this model.

**SUMMARY OF THE NEW UNIVERSAL VISCOELASTIC MODEL**

The basic universal viscoelastic model can be characterized with the following equations as described in detail elsewhere.<sup>1-5</sup>

$$\frac{\sigma}{\sigma_y} = K\epsilon + A_2(K\epsilon)^2 + A_3(K\epsilon)^3 \tag{1}$$

$$K = \frac{E}{\sigma_y} \tag{2}$$

$$A_2 = \frac{(3 - 2K\epsilon_y)}{K^2\epsilon_y^2} \tag{3}$$

$$A_3 = \frac{(K\epsilon_y - 2)}{K^3\epsilon_y^3} \tag{4}$$

$$\sigma_y = \frac{\beta}{t_y^n} \tag{5}$$

$$t = \frac{\epsilon}{\dot{\epsilon}_i} \tag{6}$$

$$\epsilon_y = \epsilon_\infty + \epsilon_0(1 - e^{-\gamma\dot{\epsilon}_i}) \tag{7}$$

where

- A<sub>2</sub>, A<sub>3</sub>, . . . , A<sub>i</sub> = variable constants for a series of strain rates for the same polymer formulation
- E = elastic modulus, psi
- K = ratio of modulus to the yield strength that is assumed to be a constant for all strain rates
- n = efficiency of yield energy dissipation
- t = time to achieve a strain  $\epsilon$ , min
- t<sub>y</sub> = time to yield, min
- β = energy dissipation constant
- ε = characteristic strain
- ε̇<sub>i</sub> = characteristic strain rate
- ε<sub>y</sub> = yield strain
- ε<sub>∞</sub> = limiting strain to yield when the strain rate approaches an infinitely small value (ε̇<sub>i</sub> → 0)
- ε<sub>0</sub> = limiting additional component of strain to yield when the strain rate approaches an infinitely large value (ε̇<sub>i</sub> → ∞)
- γ = strain rate constant for yield strain
- σ = characteristic stress, psi
- σ<sub>y</sub> = engineering yield stress, psi

According to Brown<sup>17-19</sup> and several other authors,<sup>15,20</sup> K = E/σ<sub>y</sub> is normally a constant for a given polymer formulation that typically ranges from 40 to 60. Also note that the stress σ from eq. (1) reduces to

$$\sigma \rightarrow E\epsilon \text{ as } \epsilon \rightarrow 0$$

Thus eq. (1) reduces to the standard equation to determine the elastic modulus at very low strains.

If Kε<sub>y</sub> ≤ 3, then the two conditions required to evaluate the constants A<sub>2</sub> and A<sub>3</sub> in eq. (1) were as follows.

- By definition: σ = σ<sub>y</sub> when ε = ε<sub>y</sub>
- Second condition: dσ/dε = 0 at σ = σ<sub>y</sub> when ε = ε<sub>y</sub>

The relationship described by eq. (5) between yield stress σ<sub>y</sub> and time to yield t<sub>y</sub> was addressed using the following simple relationship currently included in ASTM D2837-98a (Standard Test Method for Obtaining Hydrostatic Design Basis for Thermoplastic Pipe Materials): this relationship has also been used by Reinhart<sup>21</sup> to predict long-term failure stress (which is

normally close to the stress evaluated from the stress relaxation of the yield stress) as a function of time.

Note that the yield strain described by eq. (7) has the following limits:

$$\begin{aligned}\epsilon_y &\rightarrow \epsilon_\infty \quad \text{as } \dot{\epsilon}_i \rightarrow 0 \text{ (very long times)} \\ \epsilon_y &\rightarrow \epsilon_\infty + \epsilon_0 \quad \text{as } \dot{\epsilon}_i \rightarrow \infty \text{ (very short times)}\end{aligned}$$

In addition, at low strain rates or when  $\dot{\epsilon}_i \ll 1$  then eq. (7) can also be simplified using a McLaurin series expansion of the exponential term to give

$$\epsilon_y = \epsilon_\infty + \epsilon_0 \gamma \dot{\epsilon}_i \quad (8)$$

However, if

$$\alpha = \epsilon_0 \gamma \quad (9)$$

then eq. (8) can be written

$$\epsilon_y = \epsilon_\infty + \alpha \dot{\epsilon}_i \quad (10)$$

Brinson and DasGupta<sup>10</sup> point out that Crochet<sup>22</sup> predicted theoretically that the yield strain should decrease with an increase in strain rate. As indicated previously,<sup>1</sup> this author has found that  $\alpha$  is indeed negative for polyethylene. However, Malpass<sup>11</sup> and this author have found that for many ABS materials the strain to yield increases as the strain rate increases, which would make  $\alpha$  positive. In addition, Brinson and DasGupta<sup>10</sup> also found experimentally that the yield strain increased with an increase in strain rate for polycarbonate.

Combining eqs. (1)–(7) gives

$$\sigma = \beta \left( \frac{\dot{\epsilon}_i}{\epsilon_y} \right)^n [K\epsilon + A_2(K\epsilon)^2 + A_3(K\epsilon)^3] \quad (11)$$

$$\epsilon_y = \epsilon_\infty + \epsilon_0(1 - e^{-\gamma \dot{\epsilon}_i}) \quad (7)$$

or as  $\dot{\epsilon}_i \rightarrow 0$ , then substituting eq. (10) gives

$$\sigma = \beta \left( \frac{\dot{\epsilon}_i}{\epsilon_\infty + \alpha \dot{\epsilon}_i} \right)^n [K\epsilon + A_2(K\epsilon)^2 + A_3(K\epsilon)^3] \quad (12)$$

Based on eq. (11) or eq. (12) it is apparent that any tensile stress  $\sigma$  associated with a specific strain value  $\epsilon$ , including the yield strength  $\sigma_y$ , will increase with an increase in the strain rate  $\dot{\epsilon}_i$ . However, the strain to yield  $\epsilon_y$ , based on either eq. (7) or eq. (10), is only mildly sensitive to strain rate and is allowed to either increase or decrease slightly with an increase in  $\dot{\epsilon}_i$ .

It is also interesting to address the case that exists at very long times  $t$  or, using eq. (12) at very low elon-

gation rates,  $\dot{\epsilon}_i$ . For this case note that the yield strain  $\epsilon_y$  approaches a limiting value  $\epsilon_\infty$ :

$$\epsilon_y = \epsilon_\infty + \alpha \dot{\epsilon}_i \rightarrow \epsilon_\infty \quad \text{as } \dot{\epsilon}_i \rightarrow 0$$

For this case the constants  $A_2$  and  $A_3$  also approach the following values:

$$A'_2 = \frac{(3 - 2K\epsilon_\infty)}{K^2\epsilon_\infty^2} \quad (13)$$

$$A'_3 = \frac{(K\epsilon_\infty - 2)}{K^3\epsilon_\infty^3} \quad (14)$$

and eq. (12) then reduces to

$$\sigma = \beta \left( \frac{\dot{\epsilon}_i}{\epsilon_\infty} \right)^n [K\epsilon + A'_2(K\epsilon)^2 + A'_3(K\epsilon)^3] \quad (15)$$

Combining eqs. (6) and (15) gives

$$\sigma = \beta \left( \frac{\epsilon}{\epsilon_\infty} \right)^n \left( \frac{1}{t^n} \right) [K\epsilon + A'_2(K\epsilon)^2 + A'_3(K\epsilon)^3] \quad (16)$$

Again it should be noted that eqs. (15) and (16) apply only to the condition where the yield strain  $\epsilon_y$  approaches its limiting value of  $\epsilon_\infty$  as a result of the strain rate  $\dot{\epsilon}_i$ , approaching zero (0). Equation (16) can also be rearranged for creep analysis in the following form:

$$t = \left( \frac{\epsilon}{\epsilon_\infty} \right) \left( \frac{\beta}{\sigma} \right)^{1/n} [K\epsilon + A'_2(K\epsilon)^2 + A'_3(K\epsilon)^3]^{1/n} \quad (17)$$

As was indicated in a previous publication,<sup>1</sup> eqs. (15), (16), and (17) can be extremely helpful when trying to address either creep or stress relaxation at very low strain rates  $\dot{\epsilon}_i$  or at very long times  $t$ . However, eqs. (1)–(7) can also be used to describe a complete series of uniaxial constant strain rate curves for a given polymer formulation and/or processing condition as described in previous publications.<sup>1–5</sup>

By definition a straight line for secondary creep would involve the following equation:

$$\epsilon = \left( \frac{d\epsilon}{dt} \right) t + \epsilon_I \quad (18)$$

The derivative defined by the slope indicated in eq. (18) would normally require a formulation where the strain  $\epsilon$  would be a direct function of time  $t$ . Even though we do not have a relationship with strain as a function of time we do have eq. (17), which describes creep time  $t$  as a function of creep strain  $\epsilon$ . Therefore the derivative of eq. (17) gives

$$\frac{dt}{d\epsilon} = \frac{t}{\epsilon} \left[ 1 + \frac{1}{n} \left( \frac{1 + 2A'_2(K\epsilon) + 3A'_3(K\epsilon)^2}{1 + A'_2(K\epsilon) + A'_3(K\epsilon)^2} \right) \right] \quad (19)$$

The reciprocal of eq. (19) then gives the desired derivative or slope as

$$\frac{d\epsilon}{dt} = \frac{\epsilon n}{t} \left( \frac{1 + A'_2(K\epsilon) + A'_3(K\epsilon)^2}{1 + n + (2 + n)A'_2(K\epsilon) + (3 + n)A'_3(K\epsilon)^2} \right) \quad (20)$$

It is apparent that the term  $(d\epsilon/dt)t$  can be conveniently obtained from eq. (20). A rearrangement of eq. (18) allows the direct calculation of the intercept strain value  $\epsilon_I$  of the straight line as

$$\epsilon_I = \epsilon - \left( \frac{d\epsilon}{dt} \right) t \quad (21)$$

Substituting eq. (20) into eq. (21) then gives

$$\epsilon_I = \epsilon \left( \frac{1 + 2A'_2(K\epsilon) + 3A'_3(K\epsilon)^2}{1 + n + (2 + n)A'_2(K\epsilon) + (3 + n)A'_3(K\epsilon)^2} \right) \quad (22)$$

Equations (20) and (22) then represent the instantaneous slope and the instantaneous intercept at each creep strain  $\epsilon$ . It is particularly important to note that the instantaneous slope, as described by eqs. (17) and (20), is a function of creep time  $t$ , creep stress  $\sigma$ , and creep strain  $\epsilon$ , plus all the other model variables including  $K$ ,  $\epsilon_{\infty}$ ,  $\beta$ , and  $n$ . However, the instantaneous intercept defined by eq. (22) is a function only of creep strain  $\epsilon$  and the constants  $K$ ,  $\epsilon_{\infty}$ , and  $n$ . Most important, the intercept strain  $\epsilon_I$  is independent of creep stress and creep time.

It is also essential to recognize that the average values for the slope in secondary creep and the average intercept strain in secondary creep are extremely important. The average slope and intercept must be obtained by averaging over a series of equally spaced data points in the secondary slope region such that

$$\left( \frac{d\epsilon}{dt} \right)_{\text{Ave}} = \frac{\sum_{i=1}^{i=k} \left( \frac{d\epsilon}{dt} \right)_i}{k} \quad (23)$$

$$\epsilon_{IAve} = \frac{\sum_{i=1}^{i=k} \epsilon_{I_i}}{k} \quad (24)$$

It can easily be shown that all the secondary creep straight lines must pass through the same average intercept creep strain  $\epsilon_{IAve}$ , described by eq. (24) for all creep stresses. This average intercept creep strain has been designated<sup>4</sup> as the "projected elastic limit strain"

and has been found to effectively characterize the elastic component of a given viscoelastic material. It is also clear from eq. (22) that the location of this projected elastic limit is also strongly dependent on the efficiency of yield energy dissipation  $n$ , which was previously shown<sup>2</sup> to be a primary measure of the viscoelastic character of a material.

This universal viscoelastic model has also identified the estimated failure strain in creep that has been designated as the "critical creep strain" ( $\epsilon_{CC}$ ). This critical creep strain can be obtained by setting  $dt/d\epsilon = 0$  and solving the resulting equation for the strain at critical creep  $\epsilon_{CC}$ , to give

$$\epsilon_{CC} = \left( \frac{-(n+2)A'_2K \pm \sqrt{(n+2)^2A'_2{}^2K^2 - 4(n+1)(n+3)A'_3K^2}}{2(n+3)A'_3K^2} \right) \quad (25)$$

For this equation the values for  $A'_2$  and  $A'_3$  are limiting values for the constants  $A'_2$  and  $A'_3$  described by eqs. (13) and (14) at very low strain rates. Consequently, the values for  $A'_2$  and  $A'_3$  have been obtained by substituting the limiting value of the yield strain  $\epsilon_{\infty}$  for the yield strain  $\epsilon_y$  in eqs. (3) and (4). Also note that when  $n = 0$  then eq. (25) yields the limiting "critical creep strain" value of  $\epsilon_{CC} = \epsilon_{\infty}$ . Thus the greater the value of  $n$ , the greater the difference between the values of critical creep  $\epsilon_{CC}$  and the limiting yield strain  $\epsilon_{\infty}$ .

Finally, the relationship between instantaneous extensional viscosity  $\eta_E$ , the creep stress  $\sigma$ , and the strain rate  $d\epsilon/dt$  during the creep process can be defined as

$$\sigma = \eta_E \frac{d\epsilon}{dt} \quad (26)$$

The instantaneous extensional viscosity can then be obtained by rearranging eq. (26) to give

$$\eta_E = \frac{\sigma}{\left( \frac{d\epsilon}{dt} \right)} \quad (27)$$

Solving eq. (20) for the ratio of the creep strain to the creep time  $\epsilon/t$ , substituting this ratio into eq. (16), and then substituting this new equation for stress  $\sigma$  into eq. (27) yields an equation of the following form:

$$\eta_E = \lambda_E \left( \frac{d\epsilon}{dt} \right)^{n-1} \quad (28)$$

where the extensional viscosity constant  $\lambda_E$  can be shown to be

TABLE I  
Summary of Constant Strain Rate Data for ABS Material 25383-A

Crosshead speed (in./min)	Strain rate (1/min)	Yield strain	Time to yield (min)	Yield stress (psi)	Modulus (psi)	Ratio modulus/yield strength
0.02	0.001	0.0357115	35.7115	5200	266000	51.15384615
0.02	0.001	0.03677	36.7700	5230	266000	50.86042065
0.02	0.001	0.037272	37.2720	5430	275000	50.64456722
0.02	0.001	0.03575	35.7500	5340	283300	53.05243446
0.2	0.01	0.0348	3.4800	6060	296300	48.89438944
0.2	0.01	0.034375	3.4375	6030	292300	48.47429519
0.2	0.01	0.034579	3.4579	6050	296300	48.97520661
2	0.1	0.032695	0.3270	6670	310300	46.52173913
2	0.1	0.0329825	0.3298	6793	326000	47.99057854
2	0.1	0.033	0.3300	6855	322200	47.00218818
						Average 49.35696656

$$\lambda_E = \left(\frac{\beta K \epsilon}{\epsilon_\infty^n}\right) \left(\frac{1}{n}\right)^n (1 + n + (2 + n)A_2'(K\epsilon) + (3 + n)A_3'(K\epsilon)^2)^n (1 + A_2'(K\epsilon) + A_3'(K\epsilon)^2)^{(1-n)} \quad (29)$$

or with rearrangement

$$\frac{\lambda_E}{\beta} = \left(\frac{K\epsilon}{\epsilon_\infty^n}\right) \left(\frac{1}{n}\right)^n (1 + n + (2 + n)A_2'(K\epsilon) + (3 + n)A_3'(K\epsilon)^2)^n (1 + A_2'(K\epsilon) + A_3'(K\epsilon)^2)^{(1-n)} \quad (30)$$

Note that eq. (28) is very similar to the power law relationship that is so commonly used for shear viscosity as a function of the shear rate for a viscoelastic non-Newtonian fluid.

It is also important to recognize that the value for the extensional viscosity constant  $\lambda_E$  as described by eq. (29) yields essentially a constant when averaged over the strains involved in secondary creep such that

$$\lambda_{EAve} = \frac{\sum_{i=1}^k \lambda_{Ei}}{k} \quad (31)$$

Also note that the instantaneous extensional viscosity constant  $\lambda_E$  defined by eq. (29) is a function of only creep strain  $\epsilon$  and the constants  $K$ ,  $\epsilon_\infty$ , and  $n$ . Most important, this viscosity constant is independent of creep stress and creep time. This means that when all required model constants remain unchanged then the average extensional viscosity constant  $\lambda_{EAve}$  should also remain unchanged as multiple extensional viscosities are evaluated for different creep stresses.

It is also clear from eq. (29) that the location of this viscosity constant is also strongly dependent on the efficiency of yield energy dissipation  $n$ , which was previously shown<sup>2</sup> to be primarily a measure of the viscoelastic character of a material. We will expand further this important observation in the next sections of this report.

### EXPERIMENTAL MATERIALS AND TESTING MEASUREMENT CONSIDERATIONS

The two acrylonitrile-butadiene-styrene (ABS) materials evaluated in this study were provided by the GE facility in Washington, WV. These two ABS materials were designated as 25383-A (ABS-A) and LL-4102-N (ABS-N). All the test samples were prepared using a Brabender single-screw extruder using a slit die that yielded a cross section about 0.75 in. wide with a thickness of about 0.0625 in. Because this thickness normally cannot be effectively evaluated using the standard extensometers, it was decided to make tensile dumbbells with a gauge length of about 20 in. to increase the accuracy and minimize any potential gauge length error. The extruded strips were cut into tensile dogbone-shape specimens using a specially made cutting template on a TensilKut sample cutter (TensilKut, Knoxville, TN). The final dogbone-shape specimen width in the gauge length area was about 0.5 in. An Instron gear-driven testing machine was used to obtain the tensile measurements and the stress relaxation measurements for the ABS materials evaluated in this study. The creep measurements were also evaluated using a typical static tensile configuration with the lower grip load clamp capable of accepting standard scale weights to generate the tensile stress in the 20-in.-long dumbbell-shape specimens. The extension movement for creep measurements were followed using a cathetometer with a travel length of about 4.5 feet, similar to Model No. TC-II made by Titan (Buffalo, NY).

### CONSTANT STRAIN RATE RESULTS FOR ABS-A AND ABS-N

The ABS materials used in this study were each evaluated at three different strain rates (2, 0.2, and 0.02 in./min) and the resulting tensile properties are summarized in Tables I and II. The tensile measurements

**TABLE II**  
**Summary of Constant Strain Rate Data for ABS Material LL-4102-N**

Crosshead speed (in./min)	Strain rate (1/min)	Yield strain	Time to yield (min)	Yield stress (psi)	Modulus (psi)	Ratio modulus/yield strength	
0.02	0.001	0.03331	33.3100	4275	227300	53.16959064	
0.02	0.001	0.03492	34.9200	4280	230000	53.73831776	
0.02	0.001	0.03275	32.7500	4380	228600	51.19178082	
0.02	0.001	0.032335	32.3350	4270	226300	52.99765808	
0.2	0.01	0.035025	3.5025	4850	239500	49.3814433	
0.2	0.01	0.035229	3.5229	4990	241760	48.4488978	
0.2	0.01	0.034672	3.4672	4720	240000	50.84745763	
0.2	0.01	0.0346255	3.4626	4720	230770	48.89194915	
0.2	0.01	0.03432	3.4320	4775	246500	51.62303665	
2	0.1	0.03558	0.3558	5440	245600	45.14705882	
2	0.1	0.0359825	0.3598	5320	240000	45.11278195	
2	0.1	0.0356755	0.3568	5350	237930	44.4728972	
2	0.1	0.0359255	0.3593	5385	248000	46.0538533	
						Average	49.39051716

for ABS-A are summarized in Table I and the tensile measurements for ABS-N are summarized in Table II. As indicated in these tables, the average ratio of modulus to the yield strength  $K$  was about the same for both of these materials. In addition, the value of  $K = 49.4$  for these two materials was in the middle of the range of (40–60) previously reported by Brown,<sup>17–19</sup> Buchdahl,<sup>15</sup> and Robertson<sup>20</sup> for this ratio.

The data for the yield stress versus the time to yield for ABS-A and ABS-N are included in Figures 1 and 2 along with the fitting of these sets of data to eq. (5). The resulting values for the constants  $n$  and  $\beta$  for these

two materials are summarized in Table III. Plots of the yield strain versus the strain rate for ABS-A and ABS-N are included in Figures 3 and 4, respectively, along with the fit of these data to eq. (7). The resulting values for the constants  $\epsilon_\infty$ ,  $\epsilon_0$ , and  $\gamma$  needed to fit eq. (7) for these two ABS materials are also summarized in Table III. Note that the results in Figures 3 and 4 are exactly opposite, given that the strain to yield for ABS-A appears to decrease with an increase in strain rate, whereas the strain to yield for ABS-N appears to increase with an increase in strain rate. As indicated earlier, Crochet<sup>22</sup> and Brown<sup>17</sup> predicted theoretically

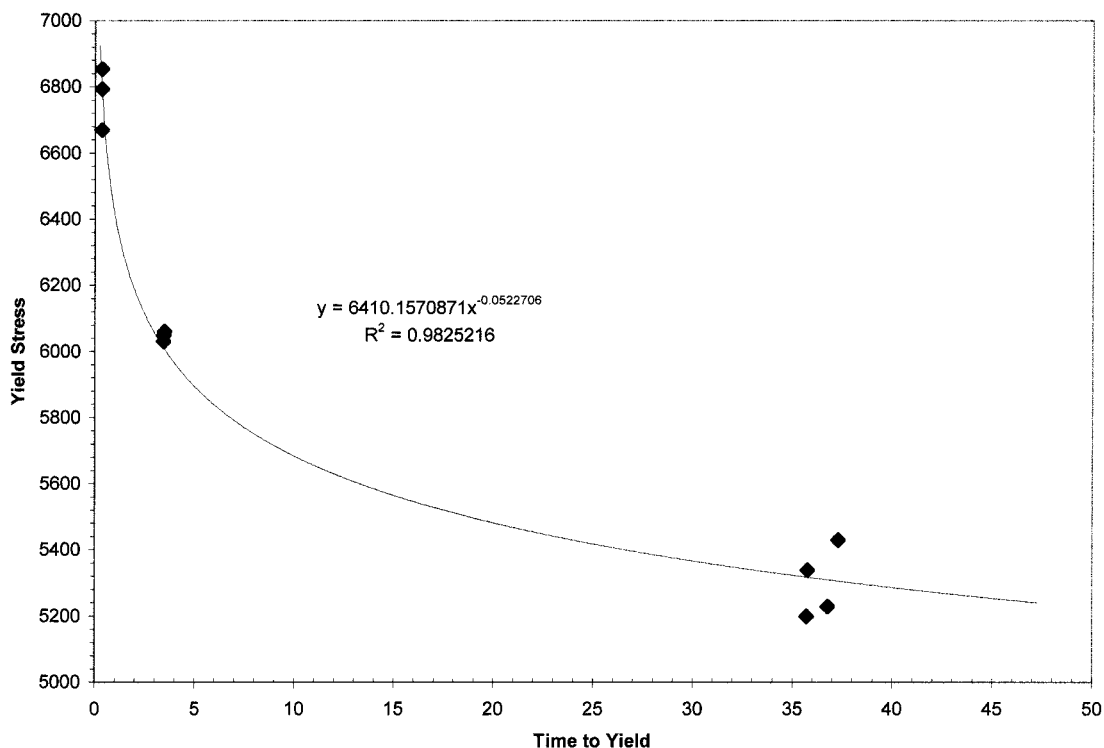


**Figure 1** Yield stress versus time to yield stress for ABS 25383-A (ABS-A).

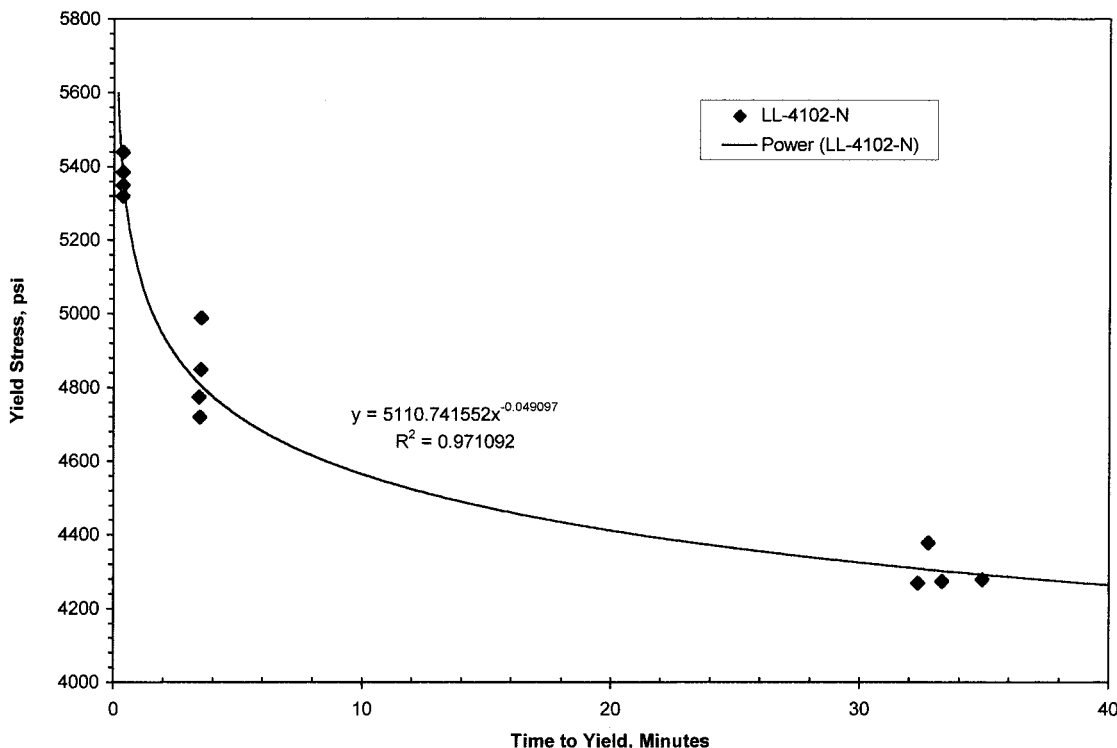


Figure 2 Yield stress versus time to yield stress for ABS LL-4102-N (ABS-N).

that the yield strain should decrease with an increase in strain rate. Previously this author<sup>1</sup> also found that the yield strain for polyethylene appears to decrease with an increase in strain rate similar to that found by ABS-A, as indicated in Figure 3. The results for ABS-N in Figure 4 appear to be consistent with the previous results found by Malpass<sup>11</sup> for another ABS material and by Brinson and DasGupta<sup>10</sup> for a polycarbonate. For these last three materials it was found that the strain to yield increased with an increase in the strain rate.

The results summarized in Table III provide a direct comparison of all the constant strain rate constants for both ABS-A and ABS-N. As already indicated in Table III the value of  $\epsilon_0$  is negative for ABS-A and positive

for ABS-N. This means that the strain to yield  $\epsilon_y$  increases with an increase in strain rate for ABS-N and decreases with an increase in strain rate for ABS-A. Although the efficiency of yield energy dissipation for both of these materials is close to the same value, the value of  $\beta$  is significantly different for these two materials. This suggests that ABS-A should be able to survive at a higher stress than ABS-N for a longer time. In general, the constants in Table III were determined entirely from constant strain rate measurements and theoretically include all the constants needed to evaluate the universal viscoelastic model for any stress or strain condition. This means that theoretically the constants included in Table III can be used to predict constant strain rate, creep, or stress relaxation conditions as needed. One additional objective of the remaining portion of this study will then be to evaluate how well this result can be achieved using experimental creep and stress relaxation measurements.

TABLE III  
Summary of Constant Strain Constants  
for Two ABS Materials

Property	ABS material	
	LL-4102-N	25383-A
Efficiency of yield energy dissipation, $n$	0.0490970	0.0522706
Beta, $\beta$ , psi	5110.74	6410.16
Epsilon infinity, $\epsilon_\infty$	0.033168	0.036575
Epsilon zero, $\epsilon_0$	0.002623	-0.003675
Gamma, $\gamma$	95.3107	73.4694
Alpha, $\alpha$	0.25000	-0.27000
Ratio modulus/yield strength, $K$	49.3905	49.3570

CREEP RESULTS FOR ABS-A AND ABS-N

The creep results for ABS-A at three different stresses (4138, 4635, and 5197 psi) are included separately in Figures 5, 6, and 7, respectively. All three of these curves have been included in Figure 8 to better elucidate the common intercept strain  $\epsilon_i$  that was identified by this author in a previous publication as the "projected elastic limit." The calculated slopes in the sec-

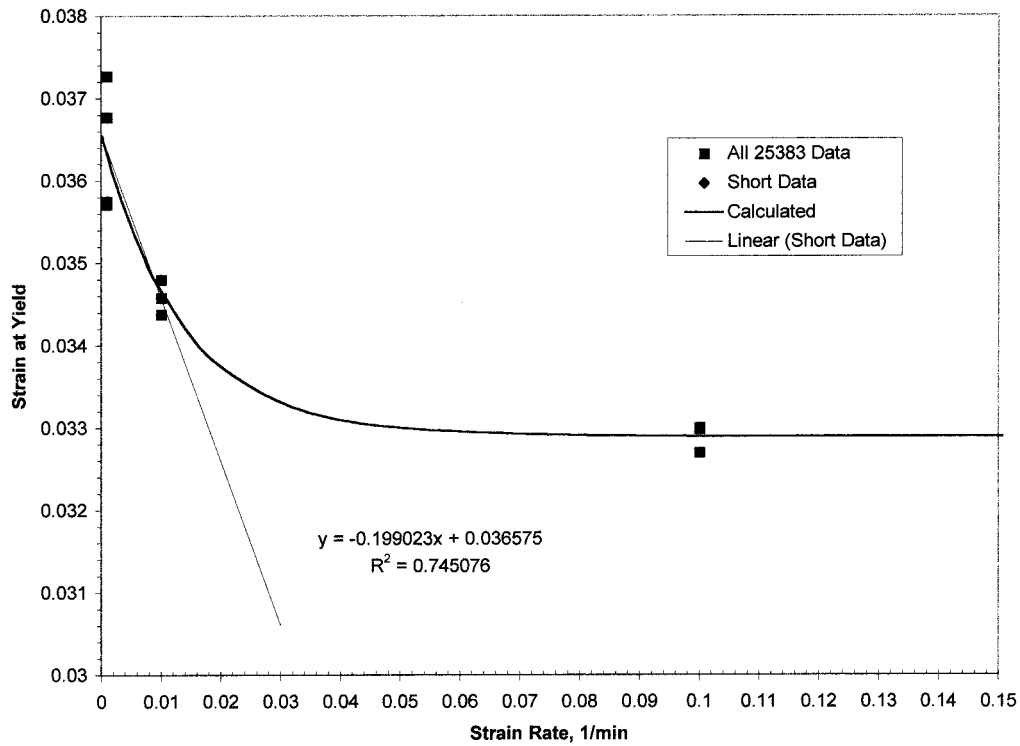


Figure 3 Strain at yield versus strain rate for ABS-A.

ondary creep regions for these different stresses have been converted to extensional viscosities using eq. (27) and plotted in Figure 9 to allow the calculation of  $\lambda_E$  and  $n$  using eq. (28).

Figures 5–7 also include the calculated fit of this model to the actual creep data using eq. (17). It is apparent that the values for  $\lambda_E$  and  $n$  can be calculated directly from eq. (28) as summarized in Figure 9 and

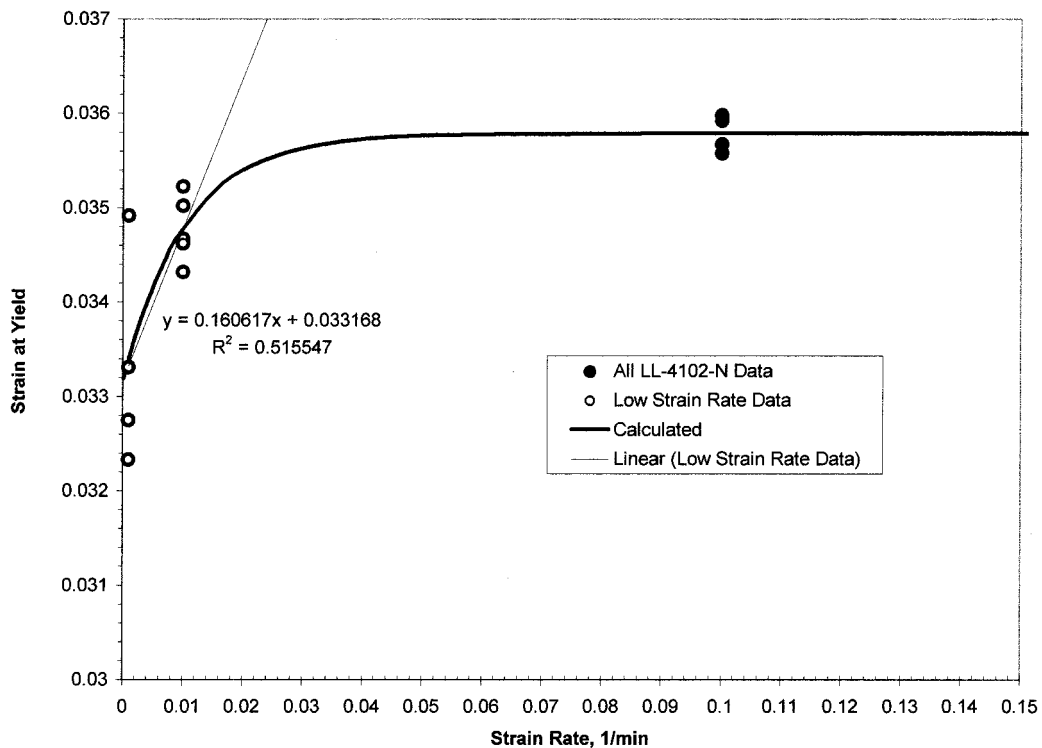


Figure 4 Strain at yield versus strain rate for ABS-N.



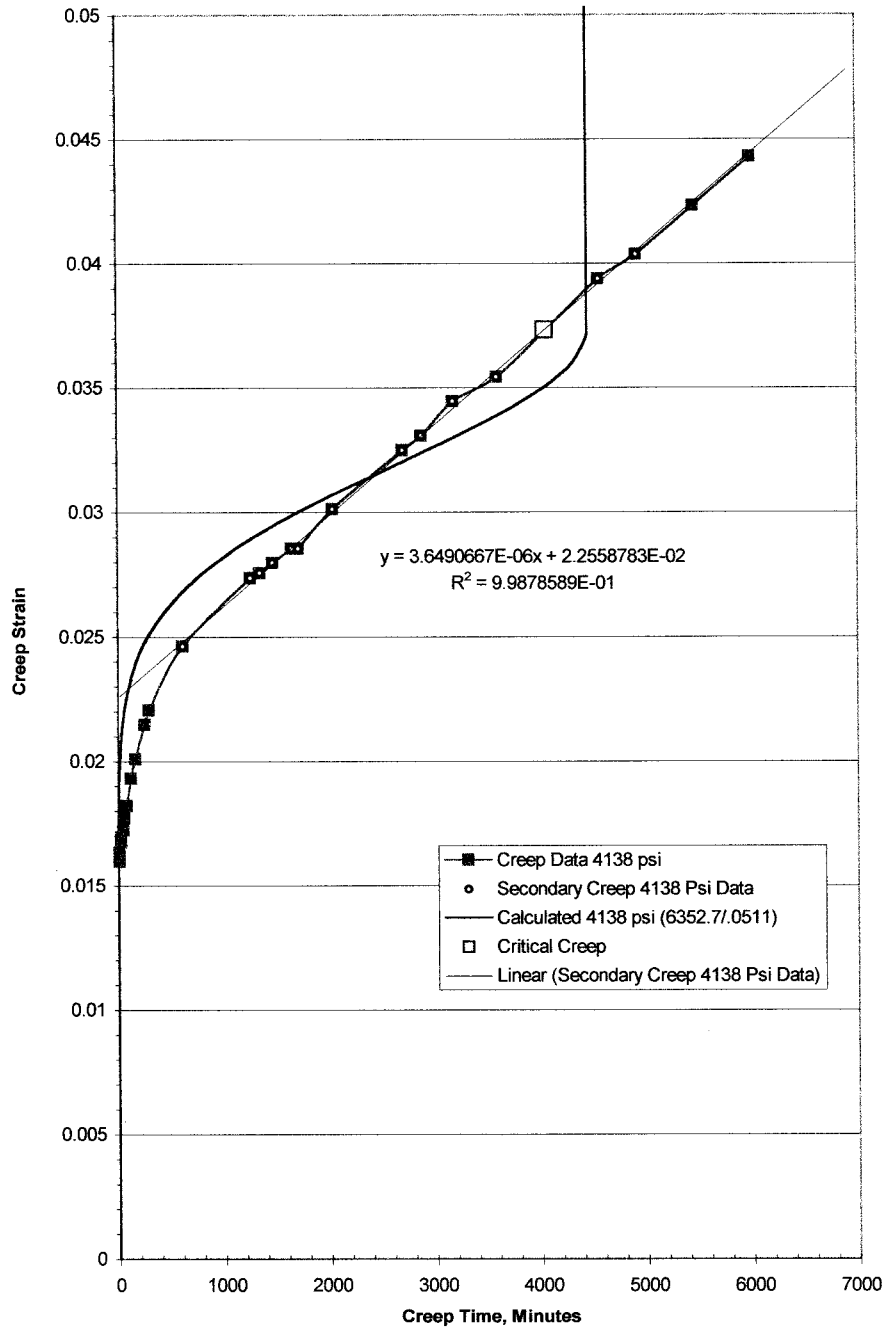


Figure 5 Creep strain (at 4138 psi) versus time for ABS-A.

Table IV. The value of  $\beta$  can then be calculated from the ratio of  $\lambda_E/\beta$  by averaging this ratio as described by eq. (30) over the range of strains in the secondary creep region.

However, it has been found to be faster and simpler to calculate and average  $\beta$  to fit creep measurements using another technique. This second approach again required the calculation of the value for  $n$  from creep measurements from eq. (28) using the creep results plotted in Figure 9. The next step involved the calculation of the strain at critical creep  $\epsilon_{CC}$  from eq. (25) using the value of  $n$  from creep measurements and the

constants for  $K$  and  $\epsilon_\infty$  from constant strain rate measurements as summarized in Table III. The resulting calculated values for  $\epsilon_{CC}$  for ABS-A and ABS-N are summarized in Table VI. The time to reach critical creep  $t_{CC}$  was then calculated by substituting the strain at  $\epsilon_{CC}$  into eq. (18) along with the straight-line constants at each stress level for ABS-A from Table IV. The resulting values for the time to reach critical creep  $t_{CC}$  at each stress level are plotted in Figures 5–7 for reference. The values of  $\beta$  for each creep stress level were then calculated from eq. (5) using the value for  $n$  from creep measurements and the calculated value for

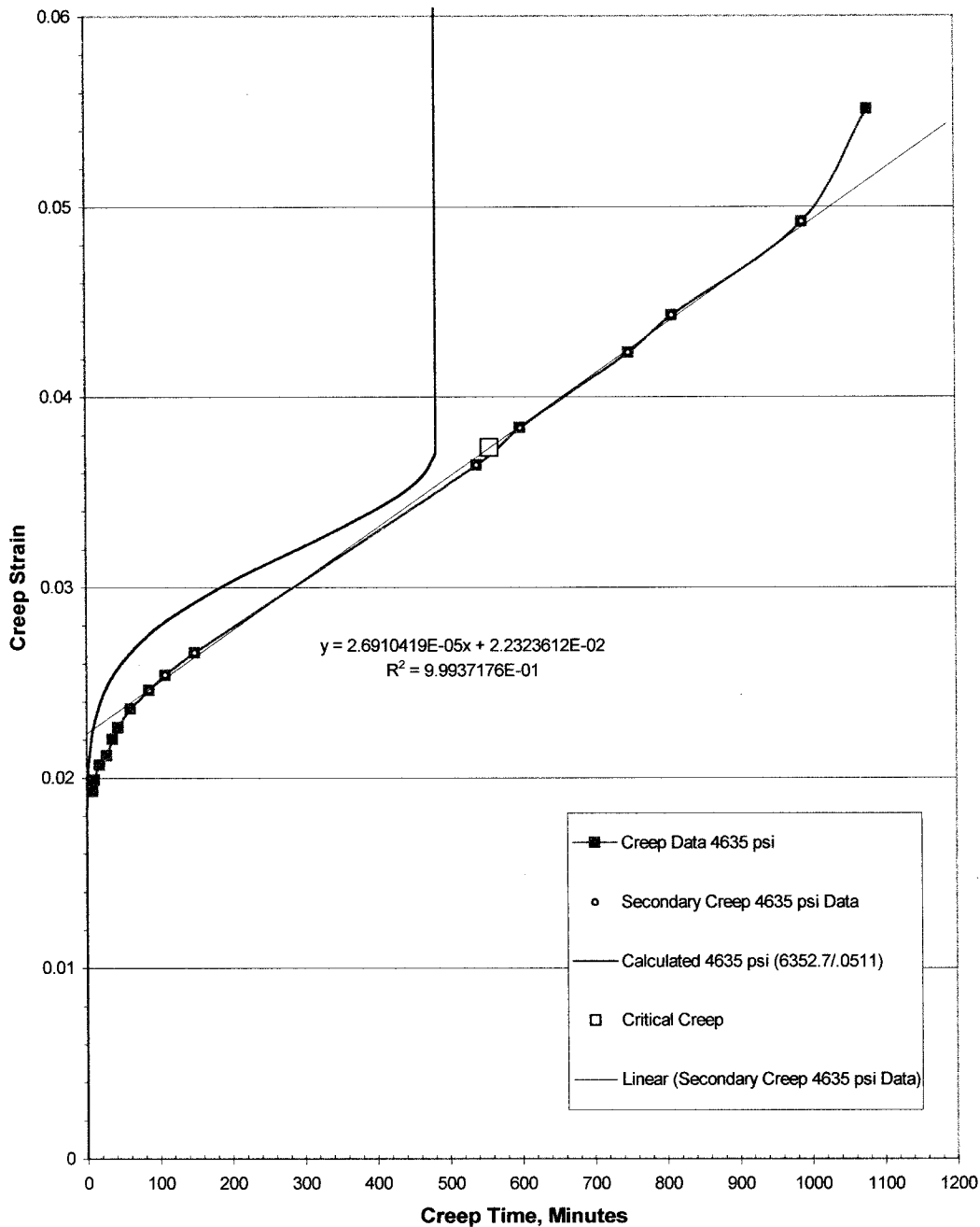


Figure 6 Creep strain (at 4635 psi) versus time for ABS-A.

the time to reach  $t_{CC}$ , as well as the known creep stress  $\sigma$ . The value of  $\beta$  that best fits the creep data was then obtained by averaging the calculated values of  $\beta$  calculated for each creep stress level. Although essentially this same value for  $\beta$  was also obtained using eq. (30), the second approach outlined here was found to be a much simpler calculation to yield a much better fit of the data.

Once the values for  $n$  and  $\beta$  were evaluated from creep measurements, then the creep model from this study as represented by eq. (17) yielded a reasonably good fit of the measured creep data for ABS-A, as

indicated in Figures 5–7. Although the actual measured slopes varied by two orders of magnitude between the three different stress levels in Figures 5–7, the average error between the measured and the calculated creep slopes was only 34.8%, as summarized in Table IV. An even lower error of 16.3% was obtained for the projected elastic limit for ABS-A between the creep measurements and calculated values from this model. For reference all of the slopes of the calculated creep curves for ABS-A are summarized in Figure 10. It is very clear in Figure 10 that all three of these calculated creep slopes intersected at exactly the

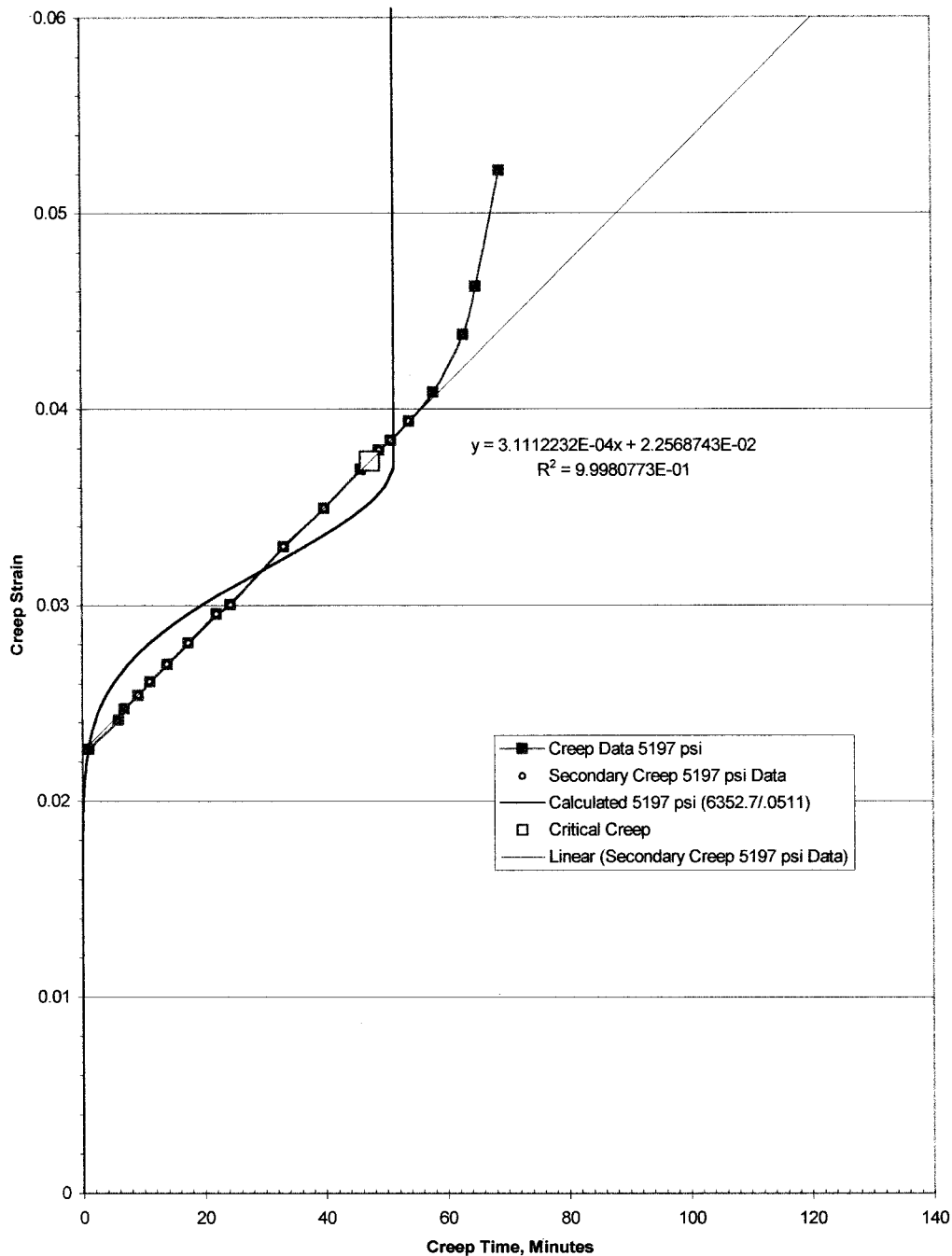


Figure 7 Creep strain (at 5197 psi) versus time for ABS-A.

same creep intercept strain, which has been designated as the “projected elastic limit,” which has been shown to be a measure of the elastic component for a viscoelastic material.

Similarly, the measured creep results for ABS-N are plotted in Figures 11–13 at three different stress levels. All three of these curves have been included in Figure 14 to better elucidate the common intercept strain  $\epsilon_I$  for ABS-N. The calculated slopes in the secondary creep regions for these different stresses have been converted to extensional viscosities using eq. (27) and

plotted in Figure 9 to allow the calculation of  $\lambda_E$  and  $n$  using eq. (28). Again for reference all of the slopes of the calculated creep curves for ABS-N are summarized in Figure 15. It is again very clear in Figure 15 that all three of these calculated creep slopes again intersected at exactly the same creep intercept strain or “projected elastic limit.” As summarized in Table V there was a better fit of the creep data for ABS-N using the model from this study as represented by eq. (17). For ABS-N the average error between the measured and calculated creep slopes was only 20%, whereas

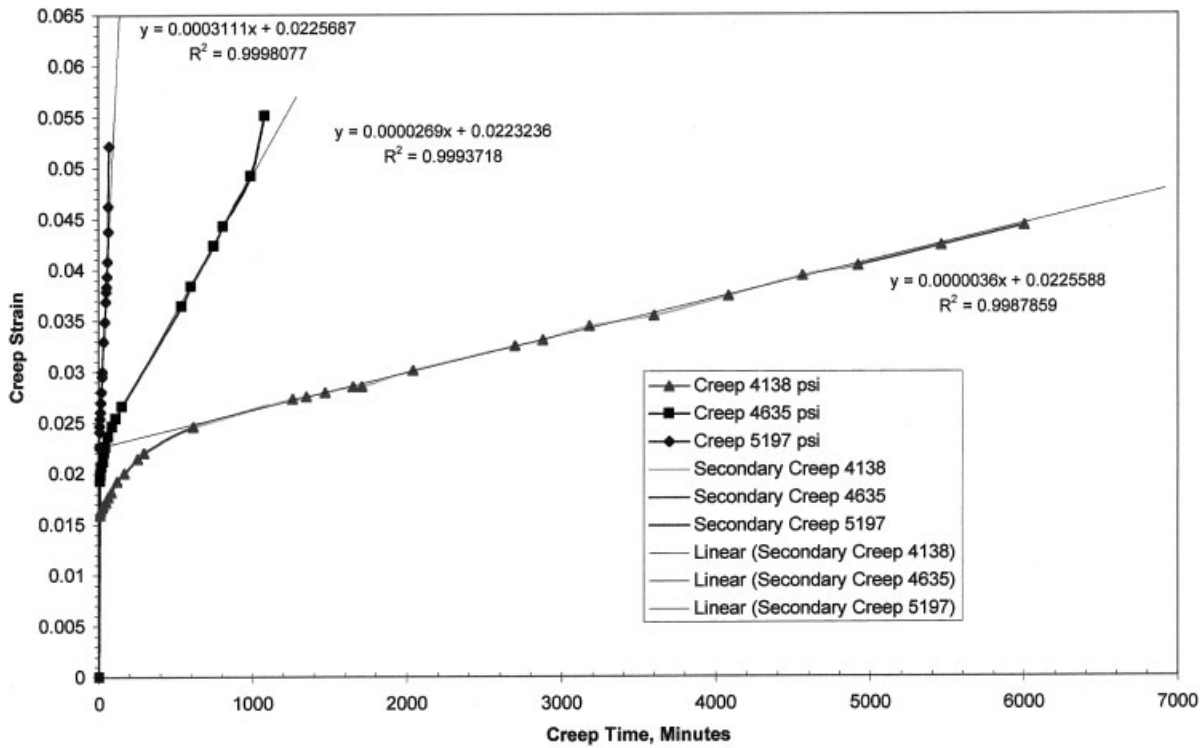


Figure 8 Creep strain versus creep time at three different stresses for ABS-A.

the average error in predicting the projected elastic limit was only 4.1%.

A direct comparison of the creep constants for ABS-A and ABS-N is summarized in Table VI. Notice that

the values for  $n$  and  $\beta$  from creep measurements for ABS-A in Table VI appear to be nearly identical to values for  $n$  and  $\beta$  from constant strain rate measurements as indicated in Table III. However, although the

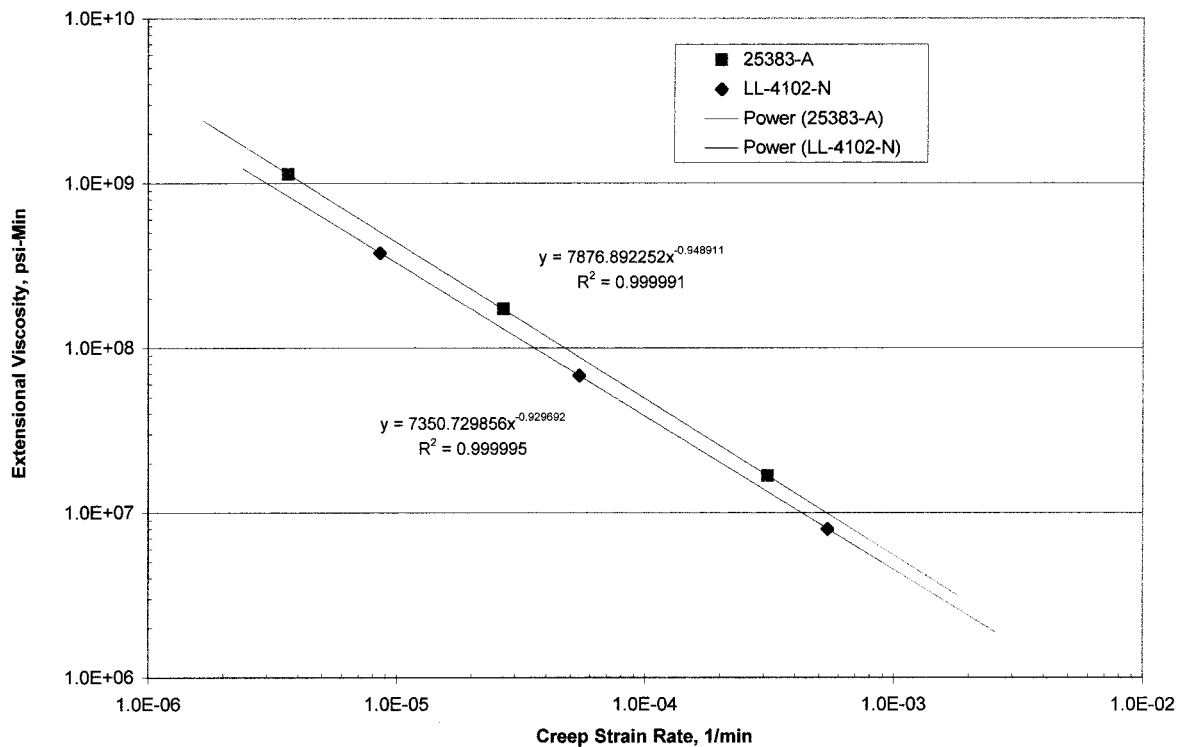


Figure 9 Extensional viscosity versus creep strain for two different ABS materials.

**TABLE IV**  
**Comparison of the Measured and Calculated Values of the Slope and Intercept for ABS Material 25383-A**

Stress (psi)	Calculated average slope (1/min)	Calculated elastic limit intercept strain	Measured elastic limit intercept strain	Measured average slope (1/min)	Secondary creep extensional viscosity (psi-min)	$n - 1 = -0.948911$	
						$n = 0.051089$	$\lambda_E = 7876.89$
4138	2.1859200E-06	0.0261389	0.0225588	3.6490667E-06	1.1339886E+09		
4635	2.0128500E-05	0.0261389	0.0223236	2.6910419E-05	1.7223812E+08		
5197	1.8909300E-04	0.0261389	0.0225687	3.1112232E-04	1.6704041E+07		
	Percentage error	Percentage error					
4138	40.1	15.9					
4635	25.2	17.1					
5197	39.2	15.8					
Average	34.8	16.3	0.0224837				

values of  $\beta$  were about the same for ABS-N for both creep and constant strain rate measurements as indicated in Tables III and VI, the values for  $n$  for ABS-N appeared to be quite different. In Table VI the value of  $n$  for ABS-N as determined from creep measurements is 37.6% larger than the value of  $n$  for ABS-A. Because the value of  $n$  for ABS-N is greater than the value of  $n$  for ABS-A, this would suggest that ABS-A should have a slightly more solidlike character than ABS-N. This result is supported in Table VI by the observation

that the projected elastic limit  $\epsilon_t$  for ABS-A is 2% greater than that for ABS-N. In addition, the extensional viscosity constant  $\lambda_E$  for ABS-A is 7.2% greater than that for ABS-N, indicating that ABS-N is slightly more liquidlike than ABS-A. Both of these observations would be consistent with the observation that the value of  $n$  for ABS-N is slightly greater than the value of  $n$  for ABS-A, suggesting that ABS-N should be more liquidlike than ABS-A. Finally, at any specific strain rate in Figure 9 it is apparent that ABS-N would

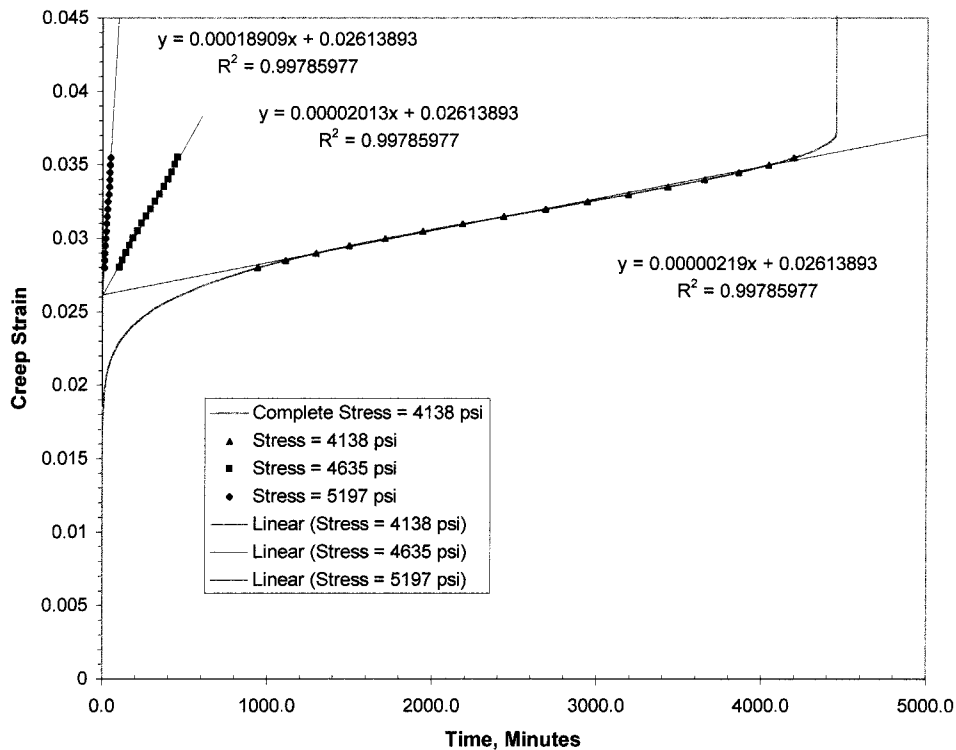


**Figure 10** Secondary creep strain versus time for ABS-A ( $\beta = 6352.7, n = 0.0511$ ).

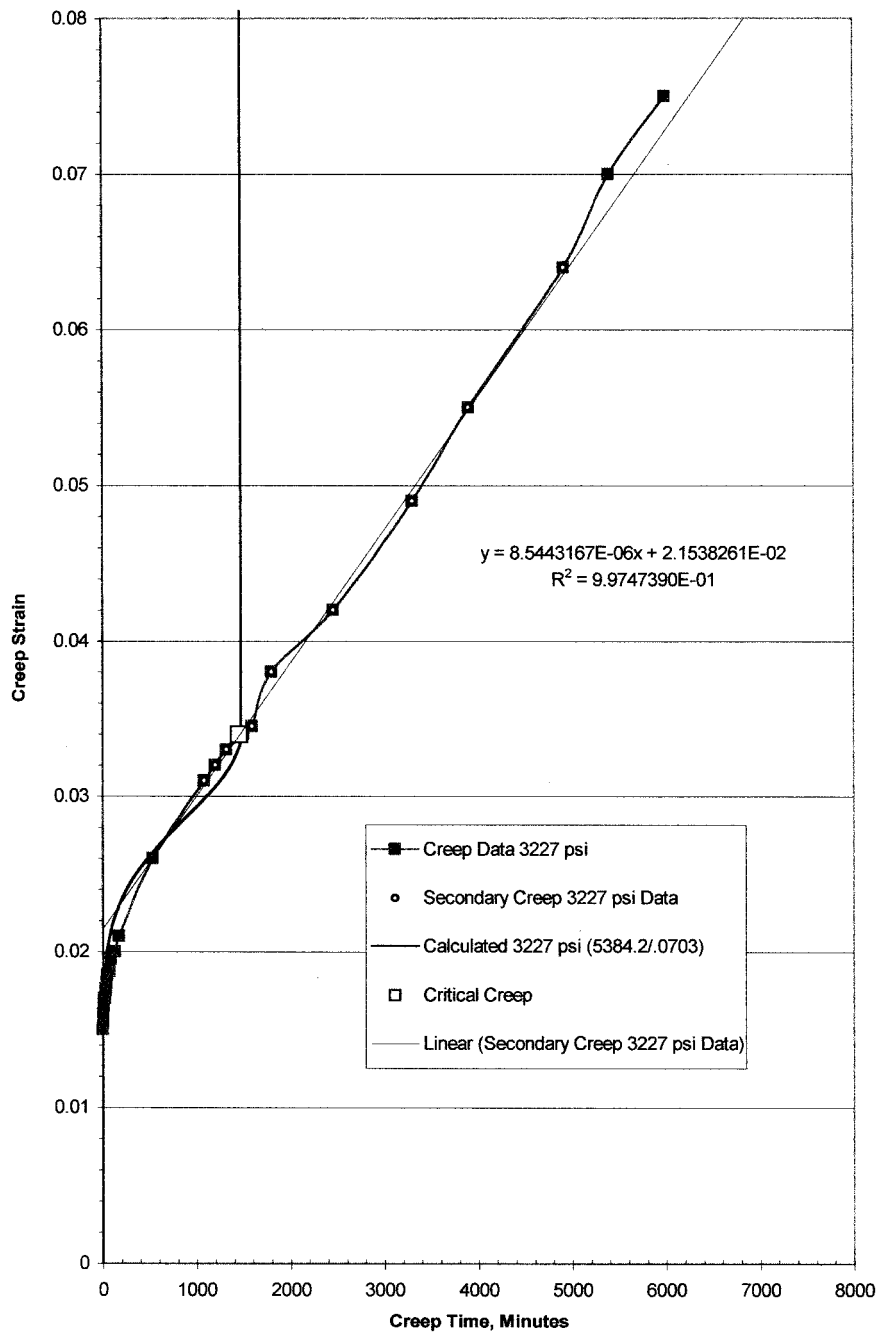


Figure 11 Creep strain (at 3227 psi) versus time for ABS resin LL-4102-N.

have a lower extensional viscosity in secondary creep than that of ABS-A. This is the best confirmation that ABS-N does in fact have a more liquidlike character than ABS-A.

However, although the data described in this study indicate that there is a difference between the viscoelastic character of ABS-A and ABS-N, the significance of this difference should be addressed in light of the practical range of the efficiency of yield energy dissipation. In a previous article by this author<sup>2</sup> as well as from similar discussions by Scott-Blair<sup>6</sup> it was found that the value of  $n$  appears to

range primarily from  $0 < n < 1$ . In this range a material would be characterized as being essentially pure elastic if it were to have a value of  $n = 0$ . A material characterized as being primarily viscous or liquid in character would have a value of  $n = 1$ . Based on these considerations it should be clear from the results in both Tables III and VI that whether  $n$  is determined from creep or constant strain rate measurements that both ABS-A and ABS-N are in general much more strongly solidlike than liquidlike. This is particularly important for failure conditions for these materials at very long times. In

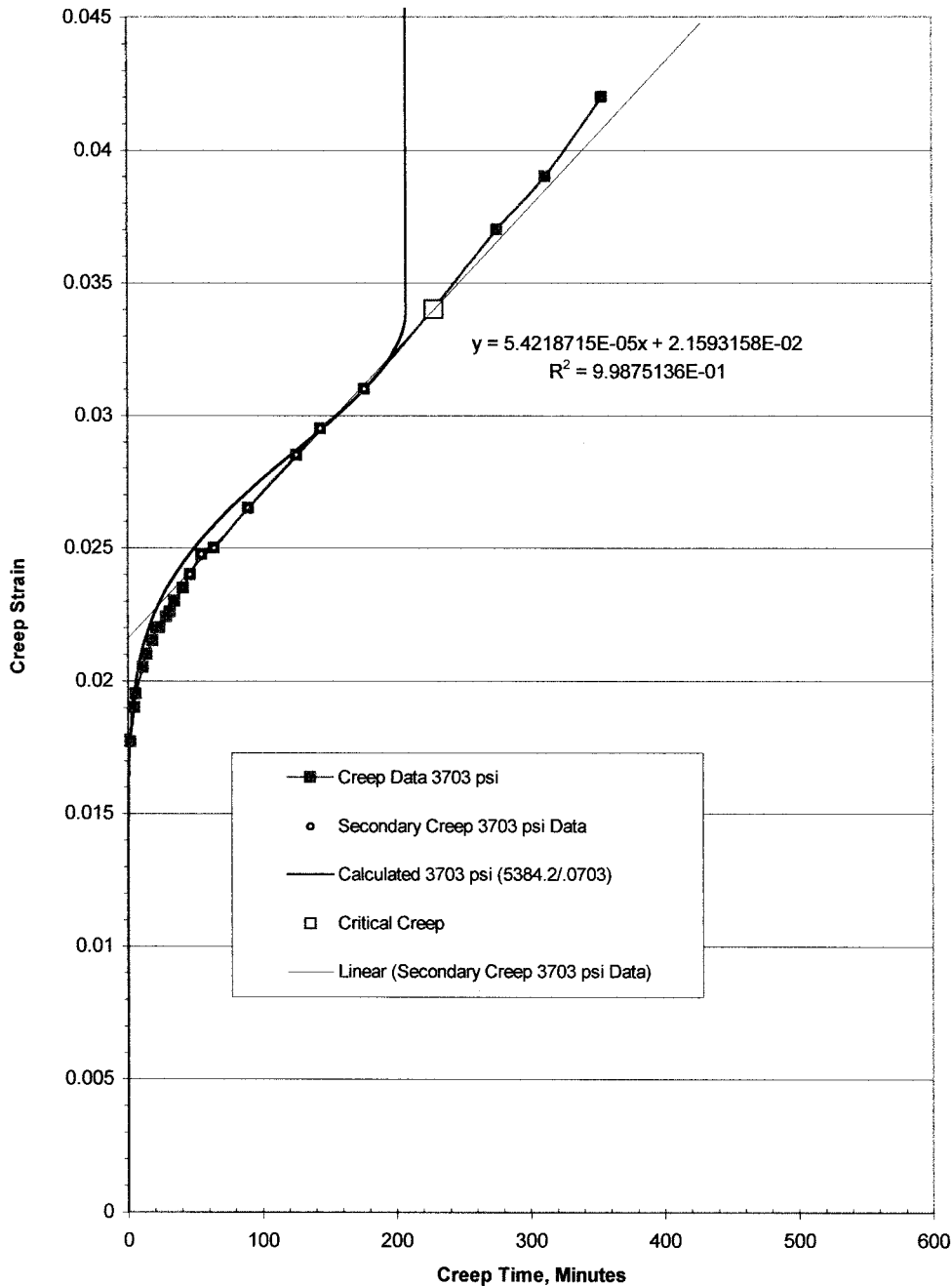


Figure 12 Creep strain (at 3703 psi) versus time for ABS resin LL-4102-N.

particular, in the next article in this series the prediction of failure using the model developed in this study will be discussed relative to the measured long-term pipe burst of these materials.

**STRESS RELAXATION FOR ABS-A AND ABS-N**

The stress relaxation results for ABS-A and ABS-N are plotted in Figure 16 at their respective yield strains to generate values for  $n$  and  $\beta$  from a direct fit of this stress relaxation data to eq. (5). For reference, the

stress relaxation of both materials in Figure 16 was initiated using a constant crosshead speed of 2 in./min until the yield strain was achieved. The results in Figure 16 indicate that the stress level was slightly higher for the stress relaxation locus of points for ABS-A than for ABS-N. Consequently, the  $\beta$  constant evaluated from stress relaxation measurements for ABS-A was found to be 35.2% higher than the value of  $\beta$  derived from stress relaxation for ABS-N. Conversely, the value of  $n$  for ABS-A was about 13.8% lower than the value of  $n$  for ABS-N. The stress relax-

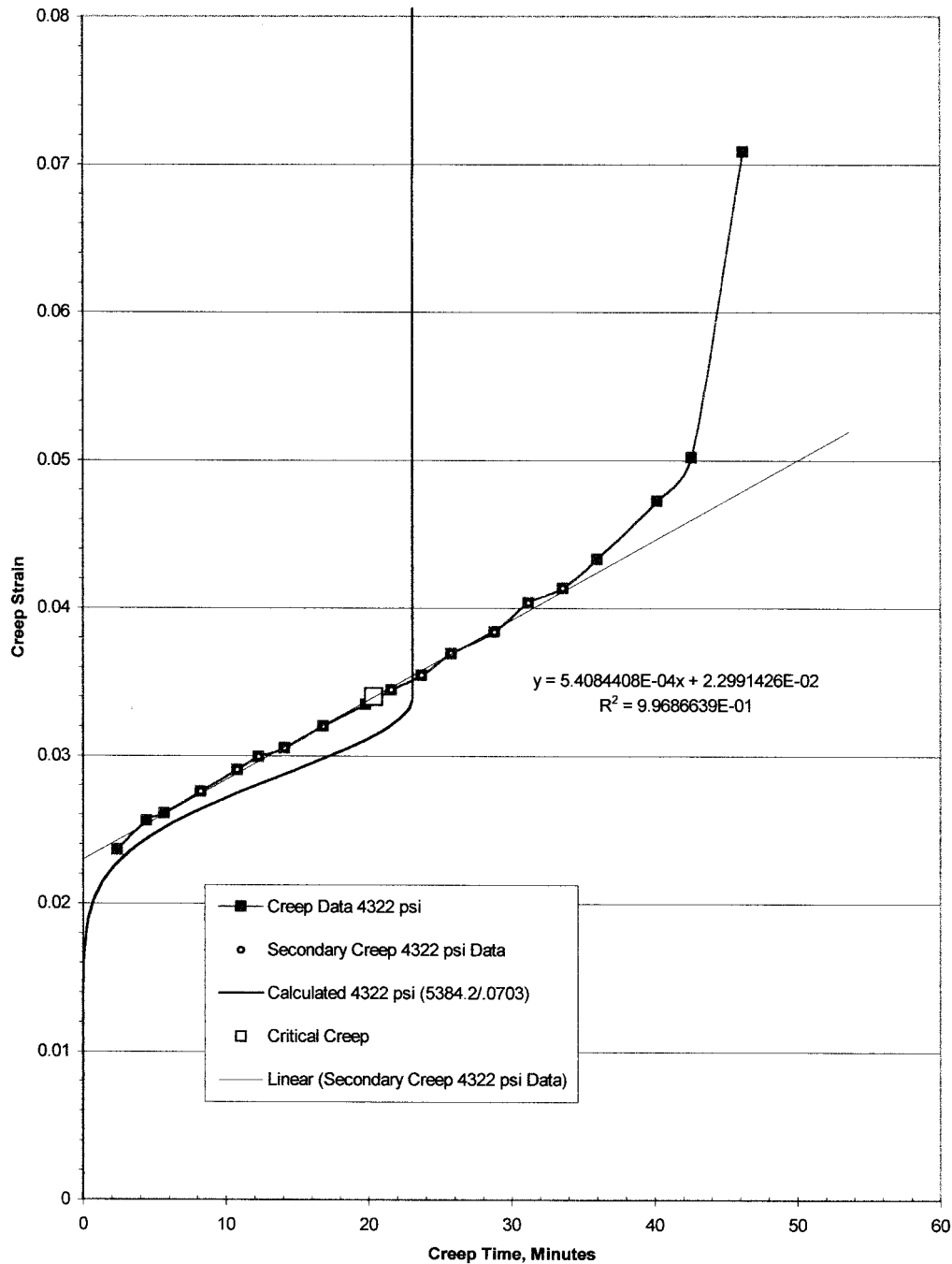


Figure 13 Creep strain (at 4322 psi) versus time for ABS resin LL-4102-N.

ation constants for these two materials are summarized in Table VII.

A comparison of the stress relaxation results in Table VII and the creep results in Table VI indicates that the values for both  $n$  and  $\beta$  were within 0.5 and 4.7%, respectively, of each other for ABS-N. However, the stress relaxation and the creep values of  $n$  and  $\beta$  were only within 15.4 and 8.7%, respectively, for ABS-A. It is not yet clear how to get these results to yield a better correlation. However, the resulting general agreement

would appear to be very desirable, given that these measurements were measured completely separately.

**COMPARISON OF THE PREDICTED FAILURE CONDITIONS FOR CREEP, CONSTANT STRAIN RATE, AND STRESS RELAXATION**

If the yield strain is considered the failure condition for constant strain rate and stress relaxation measurements and if the strain at critical creep is con-



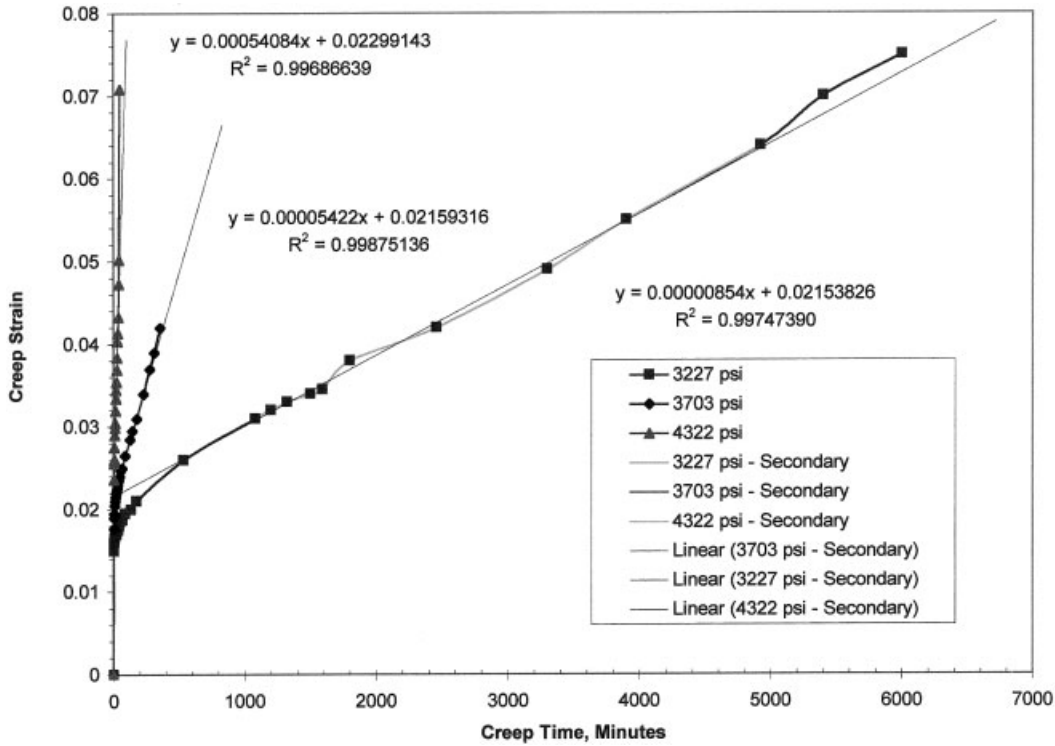


Figure 14 Creep strain versus creep time at three different stresses for ABS-N.

sidered the failure condition for creep, then these failure conditions can be compared directly, as indicated in Figures 17 and 18 for ABS-A and ABS-N, respectively. The results indicated in Figures 17 and

18 were generated using the universal viscoelastic model addressed in this study. Some observations indicated in Figures 17 and 18 would include the following:

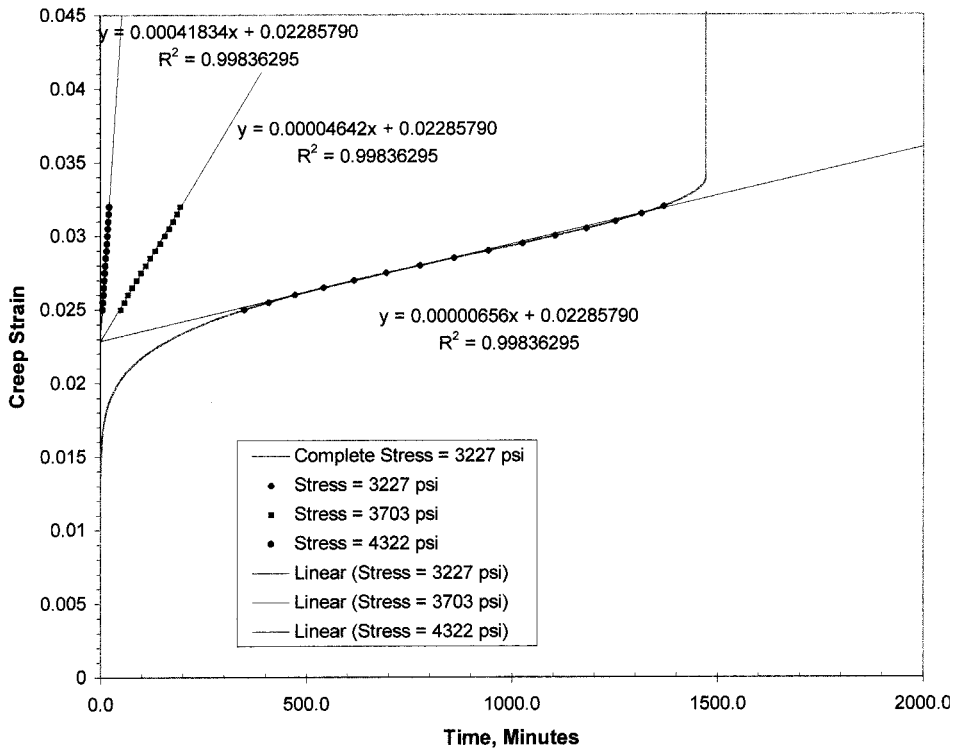


Figure 15 Secondary creep strain versus time for ABS-N ( $\beta = 5384.2$ ,  $n = 0.0703$ ).

**TABLE V**  
**Comparison of the Measured and Calculated Values of the Slope and Intercept for ABS Material LL-4102-N**

Stress (psi)	Calculated average slope (1/min)	Calculated elastic limit intercept strain	Measured elastic limit intercept strain	Measured average slope (1/min)	Secondary creep extensional viscosity (psi-min)	$n - 1 = -0.929692$	
						$n = 0.070308$	
						$\lambda_E = 7350.73$	
						$\beta = 5384.21$	
3227	6.5586761E-06	0.02285790	0.021538261	8.5443167E-06	3.7767795E+08		
3703	4.6421147E-05	0.02285790	0.021593158	5.4218715E-05	6.8297450E+07		
4322	4.1834029E-04	0.02285790	0.022991426	5.4084408E-04	7.9912126E+06		
	Percentage error	Percentage error					
3227	23.2393	6.1269					
3703	14.3817	5.8571					
4322	22.6505	0.5808					
Average	20.0905	4.1883	0.02204095				

1. The failure criteria summarized in both of these figures for the three different measurement techniques of constant strain rate, stress relaxation, and creep measurements were in remarkably good agreement. This agreement resulted even though separate and independent measurements were used for these three different evaluation techniques for both ABS-A and ABS-N.
2. The extrapolation and overlap of the constant strain rate and creep measurements for ABS-A in Figure 17 were extremely good. These results are even more remarkable because this agreement resulted from a comparison of separately measured results.
3. All of the failure criteria measurements in Figure 18 appear to merge together quite nicely. However, extrapolation to long-time failure conditions appears to give slightly different results for the three different techniques indicated.

4. The use of the results in Figures 17 and 18 to predict long-term pipe burst data will be addressed in a future companion study.

**CONCLUSIONS**

In general, the universal viscoelastic model recently published by this author<sup>1-5</sup> was found to adequately predict constant strain rate, creep, and/or stress relaxation measurements from the constants determined from constant strain rate measurements. The isolation of the elastic and viscous components for two acrylonitrile-butadiene-styrene (ABS) viscoelastic materials were also easily attainable from the constant strain rate and creep measurements using this new universal viscoelastic model.

For the two ABS materials evaluated in this study, the strain to yield for ABS-A was found to decrease with an increase in strain rate but the strain to yield for ABS-N increased with an increase in strain rate. Both the decrease in yield strain with an increase with strain rate<sup>1,17,22</sup> and the increase in yield strain with an increase in strain rate<sup>1,10,11</sup> had been previously found for other materials.

The creep results for ABS-A and ABS-N at three different stresses allowed explicit elucidation of the common intercept strain  $\epsilon_f$  for each material identified by this author in a previous publication as the “projected elastic limit.” Once the values for  $n$  and  $\beta$  were evaluated from creep measurements, then the creep version of the universal viscoelastic model yielded a reasonably good fit of the measured creep data. In general, there was a slightly better fit of the creep data and the projected elastic limit for ABS-N compared to ABS-A using the model from this study.

**TABLE VI**  
**Summary of Creep Constants for Two ABS Materials**

Property	ABS material	
	LL-4102-N	25383-A
Efficiency of yield energy dissipation, $n$	0.0703080	0.0510890
Beta, $\beta$ , psi	5384.21	6352.73
Extensional viscosity constant, $\lambda_E$ , psi-min	7350.73	7876.89
Elastic limit strain, $\epsilon_{EL}$	0.0220409	0.0224837
Epsilon infinity, $\epsilon_\infty$	0.033168	0.036575
Strain at critical creep, $\epsilon_{CC}$	0.033994	0.037337
Ratio modulus/yield strength, $K$	49.39052	49.35696656

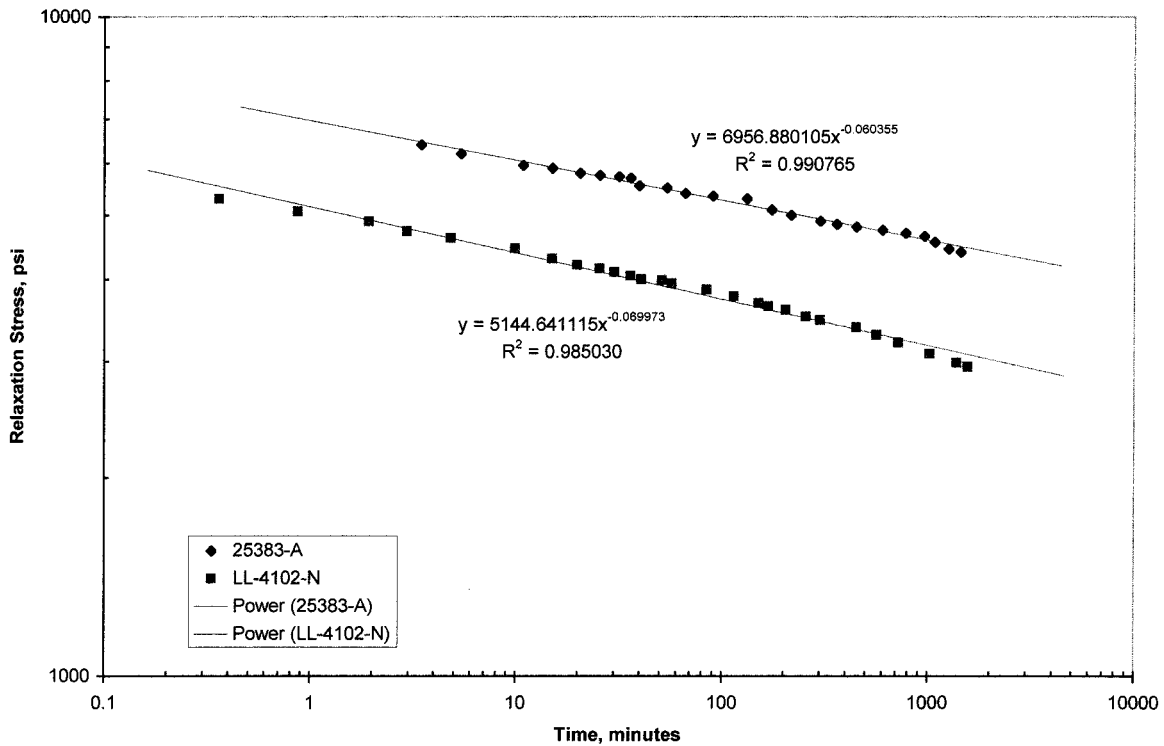


Figure 16 Stress relaxation versus time for ABS-A and ABS-N.

The values for  $n$  and  $\beta$  from creep measurements for ABS-A appear to be nearly identical to values for  $n$  and  $\beta$  from constant strain rate measurements. However, although the values of  $\beta$  were approximately the same for ABS-N for both creep and constant strain rate measurements the  $n$  values for ABS-N appeared to be slightly different. Because the efficiency of yield energy dissipation  $n$  for ABS-N was also slightly greater than the  $n$  value for ABS-A, this would suggest that ABS-A should have a slightly more solidlike character than ABS-N. In addition, the projected elastic limit  $\epsilon_f$  and the extensional viscosity constant  $\lambda_E$  for ABS-A were both slightly greater than the comparative values for ABS-N, also indicating that ABS-N was slightly more liquidlike than ABS-A. Finally, at any specific secondary creep strain rate it was apparent that ABS-

N would have a lower extensional viscosity than ABS-A. This was the best confirmation that ABS-N did in fact have a more liquidlike character than ABS-A.

Although the data described in this study indicate that there was a difference between the viscoelastic character of ABS-A and ABS-N, the significance of this difference should be addressed in light of the practical range of the efficiency of yield energy dissipation. In a previous article by this author<sup>2</sup> as well as from similar discussions by Scott-Blair<sup>6</sup> it has been found that the efficiency of yield energy dissipation  $n$  appears to range primarily from  $0 < n < 1$ . In this range a material would be characterized as being essentially pure elastic if it were to have a value of  $n = 0$ . A material characterized as being primarily viscous or liquid in character would have a value of  $n = 1$ . Based on these considerations it should be clear that whether  $n$  is determined from creep or constant strain rate measurements that both ABS-A and ABS-N are in general significantly more solidlike than liquidlike. This is particularly important for failure conditions using these materials at very long times.

A comparison of the stress relaxation results and the creep results indicates that the values for both  $n$  and  $\beta$  calculated using the universal viscoelastic model were generally in good agreement for both ABS-A and ABS-N even though these measurements were evaluated completely separately.

In general, the yield strain is often considered the failure condition for constant strain rate and stress

TABLE VII  
Summary of Stress Relaxation Constants  
for Two ABS Materials

Property	ABS material	
	LL-4102-N	25383-A
Efficiency of yield energy dissipation, $n$	0.0699730	0.0603550
Beta, $\beta$ , psi	5144.64	6956.88
Epsilon infinity, $\epsilon_\infty$	0.033168	0.036575
Epsilon zero, $\epsilon_0$	0.002623	-0.003675
Gamma, $\gamma$	95.3107	73.4694
Alpha, $\alpha$	0.25000	-0.27000
Ratio modulus/yield strength, $K$	49.3905	49.3570

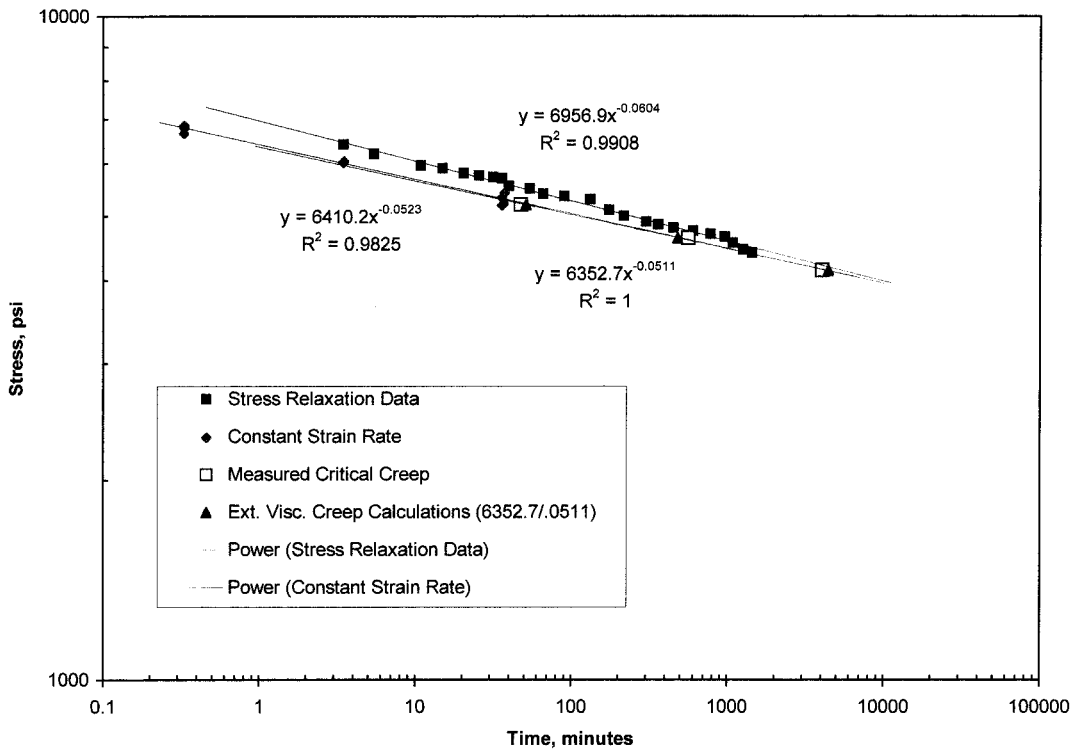


Figure 17 Constant strain rate, stress relaxation, and creep stress versus time data for ABS-A.

relaxation measurements. From this study it was found that the strain at critical creep should be considered the failure condition for creep. Using these

failure criteria for constant strain rate, stress relaxation, and creep measurements it was found that the universal viscoelastic model allowed these failure cri-

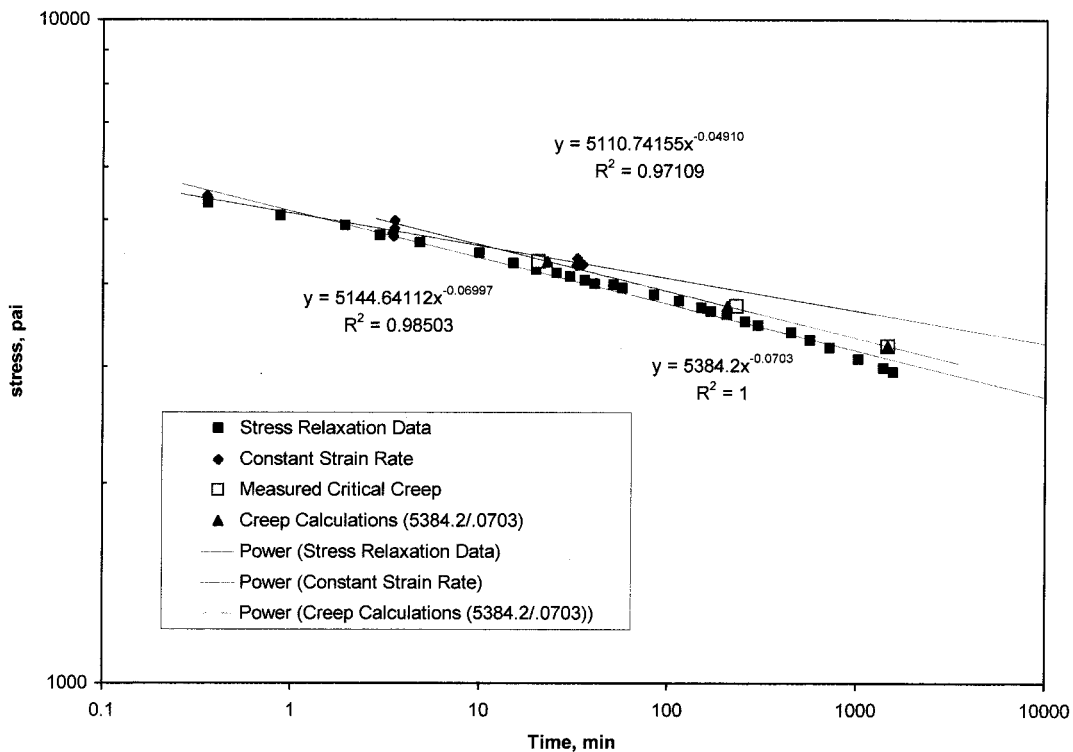


Figure 18 Constant strain rate, stress relaxation, and creep stress versus time data for ABS-N.

teria to yield remarkably good agreement. This agreement resulted even though separate and independent data were used to evaluate these three different techniques for both ABS-A and ABS-N. In particular, the extrapolation and overlap of the constant strain rate and creep measurements for ABS-A were particularly notable. These results were even more remarkable given that this agreement resulted from a comparison of separately measured results.

All of the failure criteria measurements appeared to merge together quite nicely for ABS-N. However, extrapolation to long-time failure conditions appears to give slightly different results for the three different techniques indicated. Results for constant strain rate, creep, and stress relaxation described in this study will be used to predict long-term failure in a future companion study. In the next article in this series the prediction of failure using the model developed in this study will be discussed relative to the measured long-term pipe burst for these same ABS materials.

The author acknowledges the GE Corp. for allowing publication of the constant strain rate, creep, and stress relaxation measurements for the two ABS materials 25383-A (ABS-A) and LL-4102-N (ABS-N) presented in this study. These measurements were generated by this author at GE's Washington, WV subsidiary.

## References

1. Sudduth, R. D. *J Appl Polym Sci* 2001, 82, 527.
2. Sudduth, R. D. *J Appl Polym Sci*, to appear.
3. Sudduth, R. D. *J Mater Sci* 2003, 38, 1123.
4. Sudduth, R. D. *J Appl Polym Sci* 2003, 89, 2923.
5. Sudduth, R. D. *J Appl Polym Sci*, to appear.
6. Blair, G. W. S. *J Colloid Interface Sci* 1947, 1, 21.
7. Hernandez-Jimenez, A.; Hernandez-Santiago, J.; Macia-Garcia, A.; Sanchez-Gonzalez, J. *Polym Test* 2002, 21, 325.
8. Mahfuz, H.; Zhu, Y. H.; Haque, A.; Abutalib, A.; Vaidya, U.; Jeelani, S.; Gama, B.; Gillespie, J.; Fink, B. *Int J Impact Eng* 2000, 24, 203.
9. Lee, S. W. R. *Compos Sci Technol* 1993, 49, 369.
10. Brinson, H. F.; DasGupta, A. *Exp Mech* 1975, December, 458.
11. Malpass, V. E. *J Appl Polym Sci* 1968, 12, 771.
12. Turner, S. *Br Plast* 1964, December, 682.
13. Findley, W. N. *Polym Eng Sci* 1987, 27, 582.
14. Seitz, J. T. *J Appl Polym Sci* 1993, 49, 1331.
15. Buchdahl, R. *J Polym Sci A* 1958, 28, 239.
16. Liu, Y.; Truss, R. W. *J Polym Sci Part B: Polym Phys* 1994, 32, 2037.
17. Brown, N. *Mater Sci Eng* 1971, 8, 69.
18. Brown, N. *J Mater Sci* 1983, 18, 2241.
19. Brown, N. In: *Yield Behavior of Polymers*; Brostow, W.; Corneliusen, R. D., Eds.; *Failure of Plastics*; Hanser: New York, 1986.
20. Robertson, R. E. General Electric Report No. 64-RL-(3580C), 1964.
21. Reinhart, F. W. *Polym Eng Sci* 1966, October, 28.
22. Crochet, M. J. *J Appl Mech* 1966, 33, 326.
23. Thorkildsen, R. L. In: *Mechanical Behavior*; Baer, E., Ed.; *Engineering Design for Plastics*; Robert E. Krieger: New York, 1975; Chapter 5.